

Review Article

Performance Analysis of Metamaterial-Inspired Structure Loaded Antennas for Narrow Range Wireless Communication

Kapil Jairath ¹, **Navdeep Singh** ², **Mohammad Shabaz** ³, **Vishal Jagota** ⁴,
and Bhupesh Kumar Singh ⁵

¹Department of Applied Science, IKGPTU, Kapurthala, Punjab, India

²Department of Applied Science, ACET, Amritsar, Punjab, India

³Model Institute of Engineering and Technology, Jammu, Jammu and Kashmir, India

⁴Department of Mechanical Engineering, Madanapalle Institute of Technology and Science, Madanapalle, AP, India

⁵Arba Minch Institute of Technology, Arba Minch University, Arba Minch, Ethiopia

Correspondence should be addressed to Kapil Jairath; jairathkapil@yahoo.com and Bhupesh Kumar Singh; dr.bhupeshkumarsingh@amu.edu.et

Received 3 April 2022; Revised 2 May 2022; Accepted 5 May 2022; Published 19 May 2022

Academic Editor: Punit Gupta

Copyright © 2022 Kapil Jairath et al. This is an open access article distributed under the Creative Commons Attribution License, which permits unrestricted use, distribution, and reproduction in any medium, provided the original work is properly cited.

Nowadays, the demand for low-cost, compact, and interference rejected antennas with ultrawideband capability has been increased. Metamaterial-inspired loaded structures have capability of providing exceptional solutions for narrow range wireless communication and low consuming power while transmitting and receiving the signal. It is a difficult task to construct ideal metamaterial-inspired antennas with a variety of features such as extremely large bandwidth, notching out undesirable bands, and frequency. Metamaterial-inspired structures such as SRR and CSRR, and triangle-shaped TCSRR are most commonly used structures to achieve optimized characteristics in ultrawideband antennas. In this paper, an extensive literature survey is accomplished to get conception about metamaterial-inspired patch antennas. This review paper elucidates variants of metamaterial-inspired structures/resonators utilized in order to acquire sundry applications such as WiMAX, WLAN, satellite communication, and radar. Various researchers have used different methodology to design, stimulate, and analyze the metamaterial-inspired structure loaded antennas. Also, the results of different metamaterial-inspired antennas such as bandwidth, gain, return loss, and resonant frequency have been also represented in this paper. This manuscript also gives brief introduction about the metamaterial, its types, and then its application in microstrip patch antenna over the last decade. This manuscript throws light over the various studies conducted in the field of metamaterial-inspired antenna in the past. It has been seen that with the inclusion of metamaterial in conventional antenna, various characteristics such as impedance bandwidth, reflection coefficient, gain, and directivity have been improved. Also, frequency rejection of narrow bands which exists in ultrawideband frequency range can be done by embedding metamaterial-inspired structures such as SRR and CSRR.

1. Introduction

Nowadays, wireless communication networks which include mobile, WLAN, WiMAX, and others are in high demand. During the last decade, there has been vast growth in the area of wireless technology to fulfil the growing demand of radio communication. Antenna engineering is a crucial aspect of wireless technology, as wireless communication would be impossible without precise antenna placement. Antenna can also define in terms of IEEE standard as a mean for emitting as

well as collecting radio waves. Basically, an antenna is essentially a connection between free space and an emitter or collector [1]. Figure 1 depicts the classification of different types of antennas.

From the wireless communication technology and environmental point of view, microstrip patch antenna (MSA) is an antenna which fulfils all the requirements very well such as cost effective, easy to manufacture, light weight, and low profile. [2]. Rectennas, also known as rectifying antennas, are an essential part in many energy and wireless power transfer (WPT) systems. In the particular case,

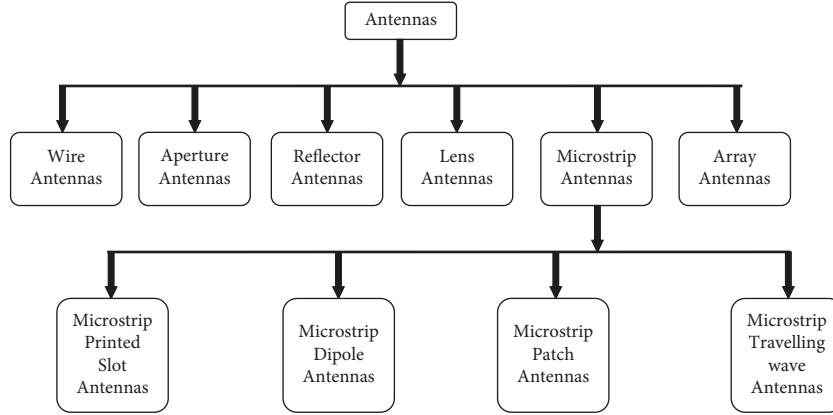


FIGURE 1: Classification of antennas.

rectennas have a wide range of antennas. Array designs include patch antennas, linearly polarized antennas, quiver antennas, and fractal antennas [3, 4]. Microstrip patch antennas (MSAs) have found diversified applications in the microwave communication system. Deschamps G. A. was the first to suggest the notion of microstrip antenna in 1953 [5]. Nevertheless, Munson [6] and Howell [7] developed practical microstrip antennas in the 1970s. The dielectric substrate is positioned between the radiator and the ground plane of a three-layered microstrip patch antenna. The radiator of radio waves can have any shape and be made up of conducting material such as copper, nickel, tin, aluminium, or gold. The materials such as FR-4 epoxy, Teflon, Polyester, Rogers RT-Duroid, Arlon, and Glass can be used as dielectric substrate as per antenna design requirement. For better performance, the dielectric constant (ϵ_r) typically ranges from $2.2 \leq \epsilon_r \leq 12$. Besides the numerous advantages of microstrip antennas, there are some drawbacks of microstrip antennas such as low power handling, low gain, extraneous radiation from feeds, low efficiency, and narrow impedance bandwidth [8]. Rectenna systems should be evaluated on the basis of their efficiency at specified input power levels, as well as their compactness [9, 10]. In order to overcome these drawbacks, various artificial materials, for example, AMC, HIS, EBG, and metamaterials (MTMs), have been used. In past few years, [11] metamaterials became most popular among research fraternity and have been widely used in antenna engineering field.

To begin with MPA design, we have to select firstly a central frequency, at which an antenna will resonate, and a substrate medium. The frameworks of radiating patch of antennas are calculated by using following equations [12, 13].

Width:

$$W = \frac{C}{2f_0 \sqrt{(\epsilon_r + 1)/2}} \quad (1)$$

Effective refractive index:

$$\epsilon_{\text{eff}} = \frac{(\epsilon_r + 1)}{2} + \frac{(\epsilon_r - 1)}{2} \left[1 + 12 \frac{h}{w} \right]^{-1/2}. \quad (2)$$

Effective length:

$$L_{\text{eff}} = \frac{C}{2f_0 \sqrt{\epsilon_{\text{eff}}}}. \quad (3)$$

Length extension ΔL :

$$\Delta L = 0.412h \frac{(\epsilon_{\text{eff}} + 0.3)(w/h + 0.264)}{(\epsilon_{\text{eff}} - 0.258)(w/h + 0.8)}. \quad (4)$$

Actual length of the patch:

$$L = L_{\text{eff}} - 2\Delta L. \quad (5)$$

Metamaterials are complex materials that have been constructed in an unnatural way to exhibit extraordinary electromagnetic properties not present in nature. These materials often obtain their unusual properties from the artificially designed structure rather than their composition, by including inhomogeneities to ratify the effective macroscopic behaviour. The permittivity and permeability are the main properties which are considered while designing the structure. The effective values of permittivity and permeability can be negative, or one of them is negative while other is positive [14]. Furthermore, metamaterials can display substantial field localization and strengthening, allowing them to be utilized to escalate sensor selectivity for recognising irregular substances and detecting enormously small concentrations of analysis [15]. Numerous novel or upgraded metamaterial applications were proposed recently based on this property. Metamaterials can be recommended to be used in place of metallic components in surface Plasmon resonance sensors in order to improve sensing performance [16] and metamaterials have also been examined as high-frequency sensors [17]. Shreiber et al. [18] combined a metamaterial lens with a microwave non-destructive evaluation sensor, and researchers were able to identify material faults as small as a wavelength. He et al. [19] studied different modes of a 2D subwavelength resonator at which it resonates, and they found that it was appropriate for biosensing. Huang et al. [20] investigated the performance of metamaterial sensor which revealed that metamaterials may considerably advance the sensitivity and resolution of the sensors. Zheludev [21] examined the future trends in metamaterial research and stated that sensor applications are another rapidly growing area of metamaterial study.

They add new dimensionality to the design of sensors, resulting in enhanced sensitivity and simplicity of use.

Two notable recent applications are the construction of electrically compact, high-efficiency rectennas for energy generation and the WPT operation of sensor networks using unmanned aerial vehicles (UAVs). While the majority of laboratory-based but commercially available sensor nodes rely on conventional batteries or other battery storage devices that require periodic fast charging or power supply replacement, future sensors are aggressively pursuing both WPT and current wireless nonradiative voltage gain (WNPT) [22, 23]. Various types of metamaterials, for example, electromagnetic metamaterials, acoustic metamaterials, and mechanical metamaterials, are used to enhance the characteristics of conventional antennas. Conductive particles and traces are embedded in a dielectric matrix to produce electromagnetic metamaterials with zero or near-zero permeability, permittivity, and refractive index. Metamaterials are employed in microwave and optics in the form of beam steerers, antenna radomes, modulators, microwave couplers, lenses, and band pass filters. These types of MTMs influence electromagnetic waves by having a shorter wavelength than electromagnetic radiation. The categorisation of materials depending on medium properties is shown in Figure 2. The first quadrant of the figure represents “Right-Handed Material,” having both positive value of ϵ and μ , also referred “Double-Positive Material” (DPS). The composite material having less than zero values of permittivity as well as permeability falls in third quadrant and often referred as “Left-Handed Material” (LHM), Double-Negative Material (DNG), or Negative Refractive Index Material (NRIM) [24–26], while other material having single less than zero value of either permittivity or permeability is referred as Single-Negative Material (SNG) which finds place in either second or fourth quadrant. Materials with less than zero value of permittivity ϵ are known as “epsilon-negative” (ENG), and materials with less than zero value of permeability μ are known as “mu-negative” (MNG) materials.

Russian physicist Victor Veselago firstly explained theoretically the concept of backward wave propagation and negative refractive index. He elucidated the electromagnetic assets such as reverse of Snell’s law, the Vavilov–Cerenkov’s effect, and Doppler’s effect. In such negative index material (NIM), velocity of em waves can spread in the reverse direction with respect to that of energy flow [27]. Even before Veselago, L. I. Mandelshtam (1944) [28] described less than zero refraction and reverse propagation of waves in his textbook and W. Rotman [29] worked with artificial dielectric and conducting parallel plate media in 1962. However, due to lack of practical realization of concept backward wave propagation, this concept did not get much attention until 1996. In 1996, H. Pendry and his colleagues practically realized the concept of backward wave propagation by imitated a continuous media exhibiting negative permittivity “ ϵ ” [30], and in 1999, a pair of open loops printed on a dielectric substrate was proposed for achieving negative magnetic permeability “ μ ” and known as split-ring resonator (SRR) [31]. This exotic phenomenon, having

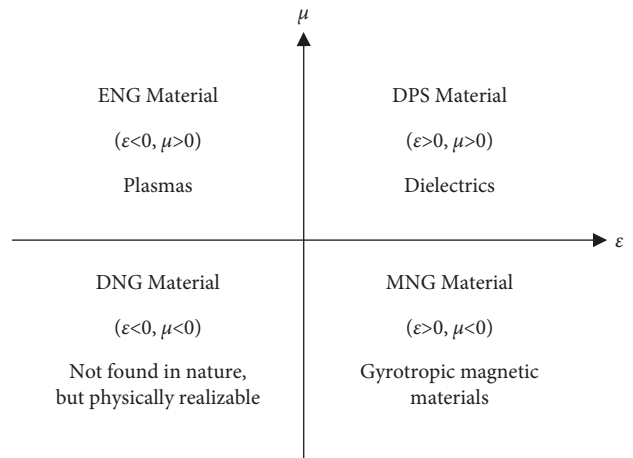


FIGURE 2: Classification of different types of electromagnetic materials based on values of permittivity ϵ and permeability μ .

applications ranging from superlens to cloaking, got interest amongst various researchers, engineers, and academicians. In 1898, Sir J. C. Bose used twisted jute fibre structure, known as artificial chiral media [32], on which first microwave experiment was conducted to emulate chiral media. D. R. Smith [24, 33] developed the first negative index medium by composing the metallic wire SRR structure, and it has been shown that the negative refractive index can exist when the real values of both electrical permittivity “ ϵ ” and magnetic permeability “ μ ” were all together less than zero. The Drude–Lorentz model has been used by various theoretical physicists to show that material exhibits the negative refractive index just above each resonance, having very small losses [34, 35]. Metamaterial-inspired SSRs and CSRRs [36] are most common candidate for UWB planar antenna technology, particularly in band rejection for narrow band interference. The split-ring metamaterial resonator and CSRR metamaterial resonators can be in square, rectangular, and circular shape as depicted in Figure 3, and the research findings are shown in Table 1. The axial magnetic field induces the currents in between the two rings of split-ring resonators which in turn yield the resonance, and the propagation signal is prohibited at that resonance frequency [42]. In the same way, complementary part of SRR, i.e., CSRRs, rejected the band pass frequency [43–45].

Metamaterials have emerged as a versatile technology with numerous uses over the last few years, and because of their small hardware footprint, they may be cost effectively embedded in various components of the wireless propagation environment, allowing for manufactured EM wave propagation control and environmental AI. With the advent of 6G broadband networks, RIS-enabled wireless communications have recently gained popularity. With the further advancement in metamaterials, it has potential or future possibilities to achieve high data transfer rate and make it suitable for 5G or 6G communications.

The sixth-generation (6G) radio wave communication systems are predicted to be life changing, progressing from “connected things” to “connected intelligence,” with much

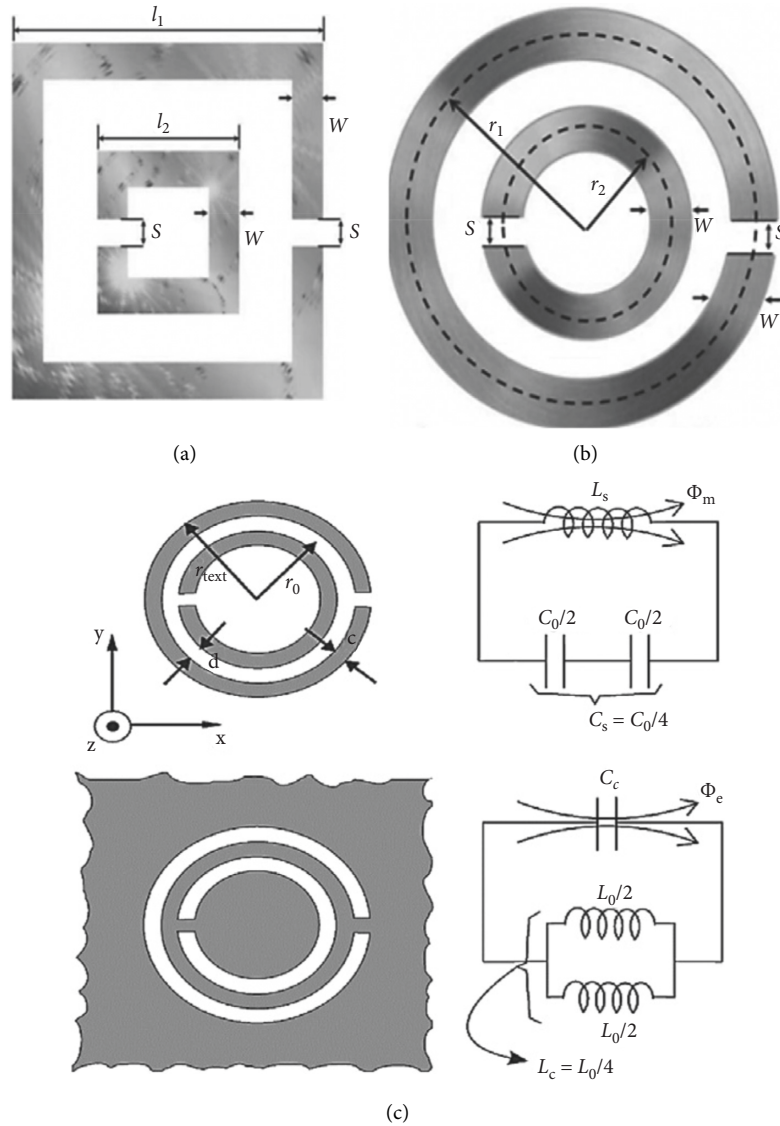


FIGURE 3: Different kind of split-ring resonators: (a) rectangular split-ring resonator (RSRR), (b) circular split-ring resonator, (c) split-ring resonator (SRR), and complementary split-ring resonator (CSRR) with its equivalent circuits [37].

TABLE 1: Major findings of the researchers on resonators.

| Authors | Resonator | Major findings |
|--------------------|--|---|
| Chen et al. [38] | A pair of SRR-based metamaterial with symmetric and asymmetric couplings. | Instead of the original low-quality factor transmittance decrease, an extra transmittance peak with a higher quality factor may be visible. |
| Singh et al. [39] | In a fixed area, the inter-SRR distance and its number density were investigated. | The Q factor along with the strength of the inductive capacitive (LC) resonance of SRRs can both be controlled by altering the periodicity pc of metamaterials. |
| Melik et al. [40] | Execute the on-chip resonators, which operate at 15 GHz and have a Q factor of 93.81 and a chip size of $195 \mu\text{m} \times 195 \mu\text{m}$. | The findings revealed that using metamaterials to boost the Q factor can be accomplished in number of ways. |
| Djuric et al. [41] | Examined the consequence of AD noise on the performance of microelectromechanical (MEMS) structure. | This noise was discovered to be caused by rapid changes in the rates of contaminant molecule adsorption and desorption on the resonator's surface. |

more stringent performance expectations including very high data rates, very high energy efficiency, massive low latency control, very broad frequency bands, ubiquitous

uninterrupted global network coverage, and connected intelligence, in comparison to previous generations of radio wave communication systems. To satisfy the aforementioned

demands, artificial intelligence (AI) is a viable technology for next-generation networks. For the design and optimization of 6G with high-level intelligence, AI has been used as a new paradigm. It may be used to address NP issues including 6G's uncertain, time-variant, and complicated properties. Security and privacy, on the other hand, are of the utmost importance to 6G because attacks and malicious behaviour can do serious damage to networks. For many applications such as WiMAX, WLAN, satellite communication, and radar, this paper presents an AI-enabled intelligent architecture for 6G networks.

2. Literature Survey

Microwave WPT has been studied for UAVs from its inception and continues to pique the curiosity of those looking for completely autonomous, continuous flight platforms. These applications necessitate electrically small rectennas, especially as their diameters shrink [46, 47]. Various experts have conducted substantial study with the intention of improvement in the performance parameters of MPA, for example, return loss and gain. Metamaterials are found to be an excellent candidate for enhancing the characteristics of antenna. Metamaterials are artificially designed structures which exhibit the negative index characteristics at certain resonant frequencies. The chronology of metamaterial-inspired antennas is as follows.

Veselago et al. [14] (1968) realized that Maxwell's equations of electromagnetism will result in a negative refractive index (n) when electrical permittivity (ϵ) and magnetic permeability (μ) are both having less than zero values. Pendry et al. [30] (1998) described a photonic structure as metamaterial composed of an array of split-ring resonator and mesh wire. The photonic structure is confirmed in three ways: analytical theory, computer simulations, and experiments on photonic structure. This new structure confirms the property of negative epsilon ϵ and unwraps the new opportunity in gigahertz (GHz) devices. Smith et al. [24] (2000) found a composite system consists of a periodic group of interspaced conducting nonmagnetic SRR and continuous wires, which forms "left-handed medium." The split-ring resonator (SRR) structure lowers the resonant frequency significantly. It has been also observed that "left-handed medium" inverts the phenomenon like Doppler's effect and Snell's law.

Qu et al. [48] (2006) represented the dual-layer MSA placed over the high-impedance electromagnetic band gap substrate. The electromagnetic band gap layer is used instead of conducting ground plane. Firstly, the structure of two-layered EBG was proposed and then band gaps of EBG were determined. It has been observed that antenna performance was influenced by the two-layer EBG substrate with air gap in between, which lead to wide bandwidth (24.69%) and higher gain of 10.32 dBi. The presented antenna is fabricated and shows excellent agreement with simulated results. Boutayeb and Dendi [49] (2007) demonstrated the circular MPA and its performance combined with a novel cylindrical-shaped EBG substrate. The suggested antenna incorporated within cylindrical electromagnetic crystal

substrate is fed by coaxial probe, for improvement of antenna gain. The cylindrical EBG structure, which is made up of two periodic structures of distinct periods and is based on a mushroom-like substrate, is an arrangement of two periodic structures of different periods. The reported design is manufactured, and the measured results reveal a 2.9 dBi increase of gain.

Weng et al. [50] (2008) elucidated a new design of metamaterial-inspired antenna for achieving multiband functions. Conventional substrate is replaced by metamaterial substrate which is composed of copper grids with square lattices. The designed antenna is fabricated and tested. At 2.77 GHz, measured measurements show an 8.2 dB gain. The observed results are in good conformity with the simulated outcomes. Li et al. [51] (2008) illustrated a novel design of planar metamaterial patterned substrate-inspired rectangular MPA. With the inclusion of metamaterial substrate to conventional antenna, working bandwidth is broadened from 200 MHz to 3 GHz along with higher efficiency and lower loss. The planned antenna has been fabricated and tested. The computed findings are very similar to the simulated outcomes.

Zhang et al. [52] (2008) suggested three ultrawideband antennas with triple band-rejection characteristics. Multiple notches have been achieved by embedding split-ring slots on radiator and SRR structure near feed line. Singh et al. [53] (2010) premeditated the coplanar waveguide (CPW) fed antenna loaded with uniplanar compact PBG structure. The bandwidth is enhanced in addition to a gain of 6.45 dBi which is attained by using the designed structure in MPA. This makes antenna suitable for WiMAX and WLAN band applications. Joshi et al. [54] (2010) suggested electrically small MPA design loaded with metamaterial configuration. The proposed antenna is constructed and tested. The tested findings revealed an increased gain of 3.21 dBi and directivity of 7.8 dBi. The prototype antenna has a 512 MHz impedance bandwidth at a resonant frequency of 9.51 GHz. Singh et al. [55] (2011) elucidated the effect of parameters of different structures on the bandwidth and resonant frequency of new metamaterial structure. It has been observed that resonant frequency and bandwidth are increased by decrease in size of patch and can be used for X-band applications.

Bertin et al. [56] (2011) demonstrated a metamaterial-inspired switch beam antenna for telecommunication applications. The proposed design of antenna comprises electrically short monopole as radiators stand vertically at four corners of the grounded square board. The proposed antenna is stimulated by using the switching network. The results of fabricated antenna reveal an extensive bandwidth of 1.1 GHz. Tang et al. [57] (2011) depicted a design of triband stop (UWB) antenna. The future antenna, which is equipped with split-ring resonator (SRR) structures, filters interference with WiMAX and wireless local area networks (WLANs) and covers a large bandwidth from 3.03 GHz to 11.4 GHz along with triband notches. The simulated results of antenna show that the prototype exhibits the omnidirectional radiation performance.

Nornikman et al. [58] (2012) introduced a designing and investigation of MPA design inspired with a single

complementary split-ring resonator (SCSRR) structure. Four different structures of SCSRR are integrated in the microstrip patch antenna. From simulation results of proposed SCSRR structures, it is found that these metamaterial structures have improved the antenna characteristic return loss, radiation pattern, impedance bandwidth, and resonant frequency. Ouedraogo et al. [59] (2012) depicted a metamaterial-inspired technique for miniaturization of patch antennas. The suggested approach comprises of a single layer of CSRR, which significantly reduces the overall area of a conventional patch antenna. The bandwidths of the antennas with reduced area up to 1/4, 1/9, and 1/16 of a conventional antenna have been found to be 1.2 percent, 0.81 percent, and 0.4 percent, respectively, in contrast to 1.3 percent for the traditional antenna. The respective efficiencies of the proposed antenna are 8.7%, 49.8%, and 28.1 percent, respectively. The simulated results have been verified by fabricating the antennas, and results show good conformity with measured outcomes.

Sharma et al. [60] (2012) elucidated a dual-frequency rejection-enabled monopole antenna which is incorporated with DGS and SRR. Dual-band stop functions are obtained by etching identical vents in the ground plane and SRR on the radiator. The presented antenna is analyzed by using CST simulation software. The simulated results predict the impedance bandwidth of 7.97 GHz and gain of 7.94 dBi along with the omnidirectional radiation pattern in H-plane. Kumar et al. [61] (2012) explained the fresh design of CPW fed metamaterial antenna encumbered with CSRR structure. The simulation results demonstrate that the suggested aerial can work throughout a frequency range from 2.482 to 2.984 GHz, allowing it to be employed in WLAN applications. Chen et al. [62] (2012) discussed recent advances in metamaterial-based sensing, as well as the principle, detection mechanism, and sensitivity of three different types of metamaterials-based sensors, as well as their problems and opportunities.

Patel and Kosta [63] (2013) premeditated the double negative group (DNG) metamaterial loaded corner curtailed square patch antenna for wireless network utilisation. The inclusion of DNG metamaterial enhances the gain 10 times more than obtain in conventional antenna. The designed antenna is investigated by HFSS simulation software. The prototype antenna exhibits maximum bandwidth of about 1.44 GHz and three operating bands which makes antenna suitable for UHF and L-band applications. Gupta and Mumcu [64] (2013) proposed a small size CSRR encumbered circularly polarized patch antenna. Firstly, multiple CSRR structures are incorporated under patch which causes the 90° rotationally symmetric antenna. Further, the proposed antenna is miniaturized by vertical inductive pin loaded truncated ground plane. The designed prototype is built and analyzed. The measured findings suggest that the projected antenna can function with a radiation efficiency of 75% at 2.24 GHz.

Kurniawan and Mukhlisshin [65] (2013) presented a design of wideband truncated circular radiator antenna for wireless communication functions. CPW fed prototyped is analyzed by using Computer Aided Design (CAD). The transmitter has been observed to work in the band from 2.3

to 6 GHz. The suggested antenna was built, and the observed results confirmed the simulations. Patel and Kosta [66] (2014) elucidated a design of compact circular MPA encumbered with CSRR structure. CSRR-based metamaterial is incorporate on the base of conventional antenna which helps in achieving seven operating frequencies along with maximum bandwidth of 259 MHz. The simulated outcomes are attained by using commercially available software HFSS which reveal that the prototype can be utilized for C and X-band applications.

Wang et al. [67] (2014) described an enhanced gain composite microstrip patch loaded with metamaterial (MTM) having near-zero refractive index. ZRI metamaterial is located 42 mm on top of conventional rectangular MPA which can gather electromagnetic beam. Between the frequencies of 3.51 GHz and 3.57 GHz, the metamaterial achieves zero refraction. The designed receiver shows realized gain more than 6 dB when analyzed by using FEM-based simulation software. Patel and Kosta [68] (2014) explicated intend of meandered MPA embedded with metamaterial superstrate. Metamaterial (MTM) metallic inclusion in superstrate consists of split-ring resonator (SRR) which enhances the antenna performances. It is revealed that the projected antenna's bandwidth increases from 11% to 60% for different bands. HFSS simulator was utilized to generate the simulated results.

Islam et al. [69] (2015) proposed a novel metamaterial antenna design that exhibits UWB characteristics and offers 114 percent bandwidth concealing the band of 3.4–12.5 GHz for a VSWR < 2 and a utmost gain of 5.16 dBi at 10.15 GHz. Mitra et al. [70] (2015) described a CPW fed ring slotted antenna incorporated with slits for miniaturization of conventional antenna. Gain, efficiency, bandwidth, and directivity have all been sacrificed to meet the electrically small resonance frequency limit. Furthermore, a metamaterial superstrate is proposed to improve the performance characteristics of antennas near the electrically tiny limit. The directivity and efficiency of antenna are appreciably enhanced with the low profile metamaterial superstrate.

Ortiz et al. [71] (2015) anticipated CSRR-based metamaterial loaded dual-band rectangular-shaped MPA. The equivalent-lumped circuit model has been given which provides a simple and easy tool for designing of the dual-band antenna. This equivalent circuit model is verified by manufacturing of three antenna prototypes. It has been observed that incorporation of CSRR structure in the conventional antenna results in miniaturization resonances which leads to the dual-band miniaturized antenna. The measured results of fabricated prototyped agree well with the simulated outcomes. Dawar et al. [72] (2015) demonstrated a miniaturized design of the microstrip patch antenna inspired by a novel metamaterial structure. The suggested antenna comprises a two-segment labyrinth-capacitive loaded strip (CLS) metamaterial embedded on a substrate. The simulated outcomes are attained by means of FEM-based HFSS software. The proposed metamaterial-inspired antenna exhibits miniaturization about 72% along with reduction in bandwidth. The designed antenna can be used for GPS, WLAN, and satellite communication.

Rajeshkumar and Raghavan [73] presented a triband SRR loaded microstrip line fed antenna for WLAN and WiMAX applications. PIN diodes are used in outer split rings for achieving reconfigurability between WiMAX and WLAN frequencies. The measured results of fabricated antenna reveal impedance bandwidth of 186%, 4.3%, and 40.3% along with omnidirectional radiation pattern in H-plane. Zhu et al. [74] (2015) depicted the two designs of electrically small antenna loaded with metamaterial. In the first design of antenna, the triangular electromagnetic resonator (TER) is added to the antenna and fed by CPW. The simulated findings prove that the planned antenna can work over three bands (1.78–1.84) GHz, (2.34–3.86) GHz, and (5.75–5.87) GHz. Furthermore, antenna 2 is developed by incorporating of Complementary TER which enhances the bandwidth and shows omnidirectional radiation pattern. WLAN and WiMAX spectrum applications are compatible with both antennas. Fabrication and testing of prototype antennas has been completed. The measured findings are very similar to the simulated ones.

Rahimi et al. [75] (2016) described a method for circularly polarizing slotted MPA and investigated the influence of an SRR-based metamaterial in a slot loaded microstrip patch antenna. The suggested antenna is made up of four different parts. HFSS and CST microwave studio software are used to simulate the antenna design. The completed antenna has a gain of 2–3.5 dBi and an efficiency of above 90%, according to this letter. The measured results from building the antenna are very close to the simulated values. Alam et al. [76] (2016) examined the design of MPA with a metamaterial (MTM) unit cell. Commercial simulation software CST and HFSS are used to simulate the planned antenna. The suggested antenna has a maximum gain of 4.06 dB and is a triple band, according to the information provided in this letter. As a result, the developed antenna is suitable for DCS 1800, Bluetooth, WiMAX, and WLAN applications in both lower and upper bands.

Gao et al. [77] (2016) proposed a design MPA composed of permeability negative metamaterial (MTM) cells to get better gain and directivity of the aerial. In this design, dual-layer symmetry single-ring resonator pair (D-SSRRP) implanted on both sides of the dielectric layer increased the gain up to 2.2 dB and decreased HPBW around 20°. The designed antenna operates at 5.2 GHz and 6.2 GHz and can be used for WLAN applications. Singla and Rajput [78] (2016) proposed a design of compact dual-band metamaterial-inspired prototyped using single CSRR structures. In this paper, different SCSRR structures such as circular, triangular, square, hexagonal, and octagonal are investigated. The designed antenna attains two bands due to inclusion of SCSRR structure and chamfered hexagonal patch antenna. The designed antenna shows a miniaturization up to 76.2% and can be used for GPS, PCS, WCDMA, and Wi-Fi applications.

Muzeeb et al. [79] (2016) described the design of epsilon-negative group (ENG) metamaterial loaded monopole antenna for quadruple applications. The consequence of metamaterial on performance of conventional monopole aerial has been investigated. It is observed that performance

of traditional monopole antenna enhances and exhibits a gain up to 3.03 dBi.

Rajkumar and Kiran [80] (2016) illustrated a compact design of modified TSRR loaded metamaterial multiband antenna. With the incorporation of modified TSRR structure, the designed antenna achieves a compact size of 25.7 mm × 23.2 mm with height of 1.6 mm. The proposed antenna is simulated by the HFSS simulator, and simulated results have been verified by fabricating the designed antenna. The given antenna achieves fractional bandwidths of 9.28 percent, 74.37 percent, and 5.34 percent, respectively, making it suitable for WLAN, WiMAX, and ITU band applications. The measured findings are very close to the simulated outcomes.

Ameen et al. [81] (2017) presented a unique triple-band circular polarized metamaterial antenna design. The metamaterial antenna is built of two Composite Right/Left-Handed Transmission Line (CRLH-TL) unit cells and a circularly polarized double hexagonal split-ring resonator (SRR). CST microwave studio is used to replicate the proposed antenna. The developed antenna displays triple-band characteristics at 2.61 GHz, 4.12 GHz, and 6.24 GHz, with an impedance bandwidth of 6.54 percent, 6.61 percent, and 34.20 percent, respectively. The designed scheme is appropriate for use with WiMAX and WLAN. Yadav et al. [82] (2017) demonstrated how to design a circular microstrip patch with triple-band notches. This circular MSA is equipped with a CSRR and a microstrip feed line with an S-shaped slot. At various angles, it has been shown that symmetrical split-ring resonator pairs (SSRPs) have been adjusted to produce band stop characteristics for X-band (7.25–8.4 GHz) satellite communication. The mentioned antenna has 3 notches at 3.5 GHz, 5.5 GHz, and 7.5 GHz. The antenna is constructed and tested, and it is discovered that the measured findings agree with the simulated results.

Heydari et al. [83] (2017) proposed a metamaterial (MTM) unit cell-based dual-band monopole antenna. The proposed antenna exhibits UWB resonances with reconfigurable quality which is achieved by introducing the four switches in Ω -shaped strip layer. The designed antenna is analyzed by using HFSS software. The presented radiator is constructed and tested. It is discovered that measured outcomes are in excellent agreement with high efficiency of more than 70%. Also, the antenna displays the omnidirectional radiation pattern with peak gain of 6 dBi which makes the antenna to operate over L-band and wireless applications. Daniel et al. [84] (2017) described a redesigned bottom layer for a metamaterial-inspired SRR constrained antenna. The intended antenna is fed by CPW, which results in excellent impedance matching and a broad bandwidth. A parametric research was conducted in order to optimize the antenna. The prototype antenna exhibits an omnidirectional radiation pattern in the H-plane and a bidirectional radiation pattern in the E-plane, making it ideal for ISM, WiMAX, and WLAN band applications.

Rajkumar and Kiran [85] (2017) demonstrated metamaterial-inspired compact open SRR MPA for multiband applications. The use of open split rings as the radiating element in this design results in a compression of 52.83

percent and 38.83 percent, respectively, as compared to a ring of the same dimensions and an SRR antenna. The proposed antenna is constructed and operates at a higher frequency of 2.8 GHz, which covers WLAN applications operating at 2.4/5.2/5.8 GHz, 5.5 GHz WiMAX, and 7.4 GHz X-band. Arora et al. [86] (2017) demonstrated a strategy inspired by metamaterials for enhancing the effectiveness of patch antennas. The proposed aerial is fabricated and tested. It has been found that the designed antenna exhibits bandwidth of 780 MHz and gain of 12.1 dBi which makes it possible for antenna to be used for WiMAX band applications.

Nuthakki et al. [87] (2017) anticipated the design of monopole planar antenna encumbered with metamaterial unit cell. Four unique unit cells have been proposed which follows CRLH-TL properties and results in four open-ended metamaterial antennas, respectively. The simulated results have been verified by fabrication of four proposed antennas and compared with measured results. It is experiential that planned antenna demonstrates enhanced bandwidth of 104%, 103%, 104%, and 103% along with gain of 4.2 dBi, 4.5 dBi, 3.5 dBi, and 4.4 dBi. The projected transmitter also shows omnidirectional radiation pattern and enhanced efficiency, suitable for ultrawideband applications. Saravanan et al. [88] (2018) premeditated the design of metamaterial-inspired superstrate MPA. The planned aerial is having a square patch antenna as radiating structure and a single-layer symmetrical phi-shaped slotted metamaterial superstrate. The simulated results are obtained by using the FDTD-based simulator. It is observed that the antenna exhibits reflection coefficient of -28.64 dB along with improved gain of 7.94 dBi.

Rao et al. [89] (2018) proposed a metamaterial-enhanced coplanar waveguide (CPW) fed circularly polarized (CP) antenna. ANSYS HFSS 17 is used to assess the intended antenna. To begin, an SRR structure is integrated into the feed line, resulting in an increase in bandwidth. Additionally, a CSRR slot is inserted over the antenna's ground plane, enabling the antenna to attain notch characteristics. The measured findings of the manufactured antenna are found to be in great conformity with the simulated results, making it acceptable for WLAN, WiMAX, and satellite applications. Labidi and Choubani [90] (2018) described the enhancement of performances of loop antenna by using negative index metamaterial (NIM). The proposed antenna consists of three TZ-shaped metamaterial unit cells on Rogers RT-5880 substrate, forming metasurface which leads to further miniaturization of loaded-loop antenna. The suggested antenna is investigated by using FDTD method-based CST microwave studio. The designed antenna exhibits a bandwidth nearly 15% about the resonant frequency of one Terahertz along with high gain around 5.39 dBi as well as directivity of 5.71 dBi. Also, inclusion of metasurface enhances the radiation efficiency up to 93%.

Chaturvedi and Raghvan [91] (2019) described intend of microstrip-fed MPA encumbered with metamaterial (MTM) structure. To begin, a SRR is integrated into a patch antenna, producing a resonance frequency of 2.72 GHz. Additionally, a 0.19×0.03 mm² stub is incorporated within the SRR

structure, extending the surface current channel and shifting the resonance frequency from 2.72 gigahertz to 2.63 gigahertz. Additionally, by covering the space with denim jeans material, the resonance frequency is reduced to 2.45 GHz. According to the observed data, the antenna has a fractional bandwidth of 19.4 percent and a gain of 1.86 dBi. The planned antenna is appropriate for WBAN applications. Hasan et al. [92] (2019) describe a wireless quad-band antenna inspired by SRR-constrained metamaterials that is electrically compact. The proposed antenna is meant to be made of FR-4 dielectric material and will have a dimension of 30 mm \times 31 mm. It will have two unit cells of metamaterial that will be aligned with one another. The proposed antenna has an overall band width of 200 MHz (between 2.40 and 2.60 GHz) and 390 MHz (between 3.40 and 3.79 GHz), making it appropriate for Bluetooth (2.40 to 2.485 GHz), Wi-Fi (2.4 GHz), WLAN (2.40 to 2.49 GHz and 3.65 to 3.69 GHz), and WiMAX (3.40 to 3.79 GHz) applications. Additionally, the antenna has an average gain of 1.50 dBi, a maximum value of 2.25 dBi, and a minimum gain of 0.88 dBi.

Devana and Rao [93] (2019) demonstrated a small size planar UWB antenna with quadruple notches. The proposed antenna is 24301.6 mm³ in volume and filters four frequencies using two inverted U-shaped slots, a symmetrical split-ring resonator pair (SSRRP), and a through hole. WiMAX, C-band, WLAN, and X-band are the four bands that have been rejected. Luo et al. [94] (2020) suggested a unique low-profile monopole UWB antenna with six band notches. The proposed antenna consists of an elliptical radiator and a rectangular ground plane with six rejections in the WiMAX band (2.96–3.33 GHz and 3.73–3.8 GHz) via the use of elliptical-shaped ESRR and round-shaped RSRR, the INSAT band (4.43–4.53 GHz), WLAN band (5.37–5.57 GHz), and C-band (7.02–7.30 GHz and 7.56–8.06 GHz). According to the simulation results, the antenna exhibits a constant gain except at rejected frequencies.

N. Sharma and S. S. Bhatia [95] (2019) proposed a novel design with a printed monopole antenna with band stop characteristics. The suggested antenna is intended on the low-cost substrate FR-4 epoxy with WLAN and X-band rejected characteristics having centred frequencies at 5.4 GHz and 7.4 GHz. The dual rejected bands have been achieved by employing CSRR slot. Also, the planned antenna exhibits a maximum gain of 4.89 dBi with negative value of gain at rejected frequencies. M. Elhabchi et al. [96] (2019) presented a dual-band notched enabled ultrawideband (UWB) elliptical slotted metamaterial-inspired antenna. The proposed antenna is loaded with a dual SRR metamaterial as a defected ground plane slot (DGS) and a single SRR metamaterial as a stub on the pinnacle edge of patch. These metamaterial structures help in avoiding the interference with the unwanted WLAN band (5–6 GHz) as well as the X-band satellite communication system (7.25 to 8.39 GHz). By controlling the dimensions of metamaterial structures and slots, bandwidth of rejected bands can be adjusted. The simulated results are obtained by using CST microwave studio and HFSS and analyze the effects of SRR slots and strips.

Thakur and Singh [97] (2020) addressed a microstrip patch antenna's bandwidth improvement. It investigates the use of DGS in conjunction with parasitic elements to create a small UWB multiband antenna. The antenna is built on an RT-Duroid (5880) substrate measuring 14×25 mm². Four different antenna designs with the same dielectric substrate are compared. The antenna design features a circular slot on the patch and is aided by shorting pins, improves bandwidth. It makes advantage of irregular defective ground structure (DGS) to improve return loss characteristics, increase bandwidth, and enable multiband operation. With five resonance frequencies of 0.92 GHz, 2.36 GHz, 3.46 GHz, 4.98 GHz, and 7.9 GHz, DGS delivers wide bandwidth (80.5 percent), making it suitable for GSM (890–966 MHz), WLAN/WiMAX (2.4/3.6/4.9), and multiband applications. Alotaibi and Alotaibi [98] (2020) proposed a novel ultra-wideband planar radiator with multiband notch. Each notch is accomplished by incorporating a C-shaped slot into the radiating patch, a U-shaped slot into the microstrip line, and an L-shaped slot into the ground plane. With three rejected bands, a nearly 10 GHz operational band is obtained (2.08GHz–12 GHz) (3.28–3.91 GHz, 4.9–7.15 GHz, and 9.21–10.94 GHz). It also has an omnidirectional emission pattern, reducing interference from technologies such as WiMAX, WLAN, and X-band applications. Althwayb [99] (2021) demonstrated how to use substrate-integrated waveguide (SIW) technology to improve the radiation gain and efficiency of a metamaterial (MTM)-inspired planar antenna for sub-6 GHz wireless communication systems. MTM unit cells with series interdigital-capacitor and short-circuited spiral stub make up the antenna. The proposed antenna works in the same way as a leaky wave antenna. The input signal leaks energy as it propagates along the antenna structure in transmission mode. The antenna's performance is improved by inserting a column of metallic connectors between the MTM unit cells. The antenna's size is unaffected by this procedure. On a normal, the antenna was built. It was operated at a frequency range of 1.8 GHz from 3.0 to 4.8 GHz. The antenna's average gain as well as efficiency after SIW was 5.8 dBi and 78 percent, respectively, representing a 2 dBi and 21% improvement throughout 3–4.8 GHz. Christydas and Gunavath [100] (2021) proposed a 6 evolution small octa-band rectangular microstrip patch antenna. Multiband operations are enabled via CSRR, SRR, FR-4 dielectric substrate and C-shaped slots, which are required for all multipurpose communication systems. In addition to its compact dimensions, the proposed antenna includes 8 resonances at 2.25 GHz, 3.86 GHz, 6.94 GHz, 7.48 GHz, and 9.47 GHz, and a reasonable gain in all operational bands. All resonant bands have efficiency above 65%. The negative permittivity and permeability are extracted. The simulated and measured findings are identical. Modern multifunctional wire systems can easily fabricate and integrate the suggested RMPA.

3. Research Gaps and Future Possibilities

Numerous researchers have investigated various strategies for shrinking the size of conventional antennas while

simultaneously improving their performance characteristics such as increased bandwidth, reflection coefficient, directivity, gain, and radiation pattern. With the diverse requirements of today's wireless communication systems, it is worth noting that no single form of classic antenna is capable of addressing all of them simultaneously. However, metamaterial-inspired resonator-based antennas have been shown to dramatically improve antenna performance in comparison to conventional antennas. It is reasonable to expect that metaresonator loaded antennas will strive for miniaturization, multifunction, multiband frequency, band notching, and broadband capabilities such as 5G or 6G in the future, and metamaterials-based antennas, with their unique properties, offer a novel approach to accomplishing these goals. Thus, a better knowledge of how metamaterials work will result in more of these structures being used in future wireless antennas.

Figure 4 depicts the measured and simulated outcomes of several research studies. Figure 4(a) depicts the antenna gain for both computational and experimental reasons. Simulated and measured antenna gain is in the range of -2 to 6 dBi, which is adequate for wireless applications. When impedance mismatch occurs at lower frequencies, as illustrated above, the return loss exceeds -10 dB and the gain is significantly reduced. A similar issue occurs at 6 GHz when the antenna is mismatched, resulting in a loss of gain at the same frequency. In calculations, the antenna efficiency exceeds 70% in the UWB frequency range [82]. Figure 4(b) illustrates a comparison of the three setups' simulated return loss characteristics. Due to the impedance mismatch, configuration A does not exhibit any apparent resonance, whereas configuration B exhibits a single-band resonance at WiMAX 3.73 GHz with an impedance bandwidth of 80 MHz (3.69–3.77 GHz). The suggested antenna (configuration C) contains many resonances at 1.77 GHz, 2.61 GHz, 3.24 GHz, and 4.15 GHz. The two C-shaped slots' length has a significant effect on the multiband resonance. After the introduction of two C-shaped slots, the resonance frequency of CSRR (3.7 GHz) is shifted to 3.24 GHz. This is due to the fact that the current flow through the CSRR slots has shifted [83].

To understand the above discussed literature survey in a better way, it has been specified in Table 2. The table has been bifurcated into two categories SRR and CSRR or DGS. First 23 articles summarized in the table are classified under the SRR-based antenna which enhances the various antenna characteristics, and further 22 articles are categorised under CSRR or DGS loaded antenna for enhancement of antenna performances.

4. Discussion

From the above discussed detailed literature survey, we have observed that the return loss, impedance bandwidth, directivity, and gain are important performance parameters of antenna. These parameters should be matched with the range of resonating frequency. Generally, researchers focused on miniaturization of patch antennas without the deteriorating of other antenna performance characteristics. As a result, researchers add metamaterial into traditional

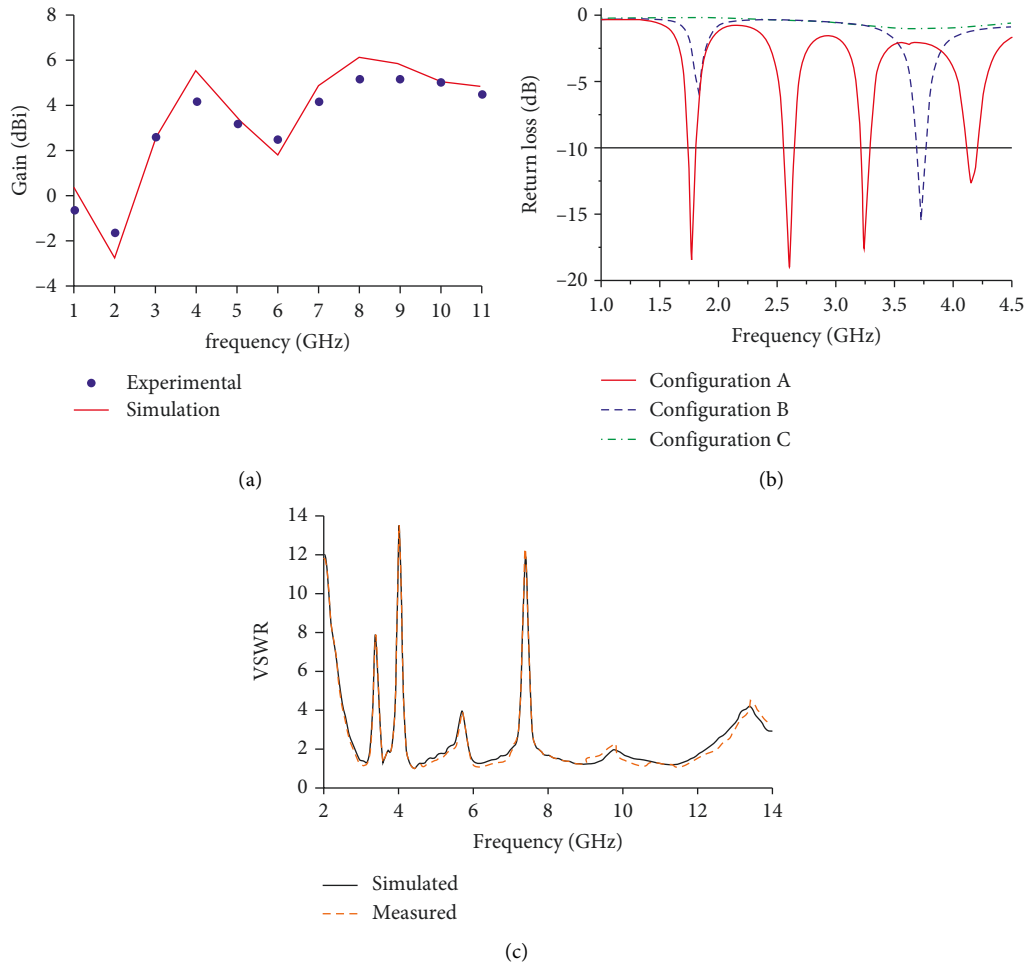


FIGURE 4: Simulated and measured results of various metamaterial-inspired antennas (a) Heydari et al. [82], (b) Daniel et al. [83], and (c) Devana and Rao [92].

patch antennas in order to recover performance metrics without increasing the patch antenna's overall size or complexity of structure. Metamaterials may be utilized for a variety of antenna functions, according to the technical requirements of the antenna design.

The reduced gain of traditional patch antennas is one of its major drawbacks. With the inclusion of metamaterial structures, the resonant frequency becomes equal to plasma frequency which results in zero permittivity or permeability and hence refractive index becomes equal to zero. Then, according to Snell's law, all outgoing radiations from the substrate will be perpendicular to the plane, and all refracted radiations will be directed in the same direction, providing a high gain and directivity. The high gain can be found by using metamaterial as unit cells of PBG [53, 76] around the radiating patch. Metamaterial substrates [51, 67] embedded in the conventional patch antenna help in getting better gain of antenna. Gain of conventional MPA can also be enhanced with using electromagnetic band gap (EBG) structures [49]. Metamaterial-inspired SRR and CSRR [75] are also effective in recuperating the gain of antenna. Miniaturisation of conventional MPA can be achieved through loading the metamaterial structures. Metamaterial loaded patch antenna

produces subwavelength at resonant modes of the conventional patch antenna. SRRs and CSRRs [59, 64] are most commonly used for size reduction of patch antenna without deforming the antenna performance parameters. The two segmented labyrinth-capacitive loaded strip (CLS) [72] metamaterial is a novel way of reducing the size of antenna. By using metamaterial as a superstrate, antenna size can also be reduced by improving other antenna parameters. Additionally, metamaterials can be utilized to increase an antenna's bandwidth and provide multiband properties. Various techniques can be employed to achieve multiple bands such as triangular electromagnetic resonator (TER) [74], different single CSRR structures (circular, triangular, square, hexagonal, and octagonal) [61], and metamaterial unit cells in the patch antenna [75]. CSRRs [58, 64] and SRRs [73] can be used for obtaining enhanced bandwidth without increasing the overall size of antennas. In ultrawideband antennas, there is need to filter out the existing narrow bands such as WiMAX, WLAN, and X-band. Metamaterial-inspired structures, for example, SRRs [57] and CSRRs [81], in addition to defected ground structures [60] can be embedded either on radiator or near the feed line to achieve desired frequency notching.

TABLE 2: Comparative analysis of various metamaterial-inspired antennas.

| Ref. | Dimensions of antenna ($L \times W \times h$) | Resonant frequency (GHz) | Return loss (dB) | Bandwidth (MHz) | Gain (dBi) | Applications |
|---|--|--------------------------|------------------|-----------------|----------------------------|-------------------------------------|
| Metamaterial-inspired SRR loaded antennas | | | | | | |
| [49] | 1.60 * 60 * 1.59 | 10.5–13 | –34 | 2500 | 8.02 | C, X, and ku-band applications |
| | 2.8 * 80 * 1.59 | 6.25–7.7 | –44.77 | 1400 | 10.32 | |
| [50] | 180 * 80 * 3.2 | 2.6 | –20 | 80 | 2.9 | S-band applications |
| | | 1.66 | –29.1 | | 5.8 | |
| | | 2.02 | –11.1 | | 0.8 | |
| [51] | 165 * 165 * 2 | 2.40 | –10.1 | ---- | 4.2 | Wi-Fi, GPS, and mobile applications |
| | | 2.48 | –11.4 | | 3.6 | |
| | | 2.77 | –33.0 | | 8.2 | |
| [52] | 12 * 16 * 0.762 | 6.66 | <–20 | 3200 | 7.14 (peak) | C-band |
| | | 7.77 | <–15 | 2900 | | |
| | PBG cell | For 3 * 8 cell | For 3 * 8 cell | For 3 * 8 cell | | |
| | 5 * 5 | array | array | array | | |
| | | 3.55 | –34.07 | 150 | | |
| [53] | With circular air gap $r = 3$ mm | For 3 * 5 cell | For 3 * 5 cell | For 3 * 5 cell | 6.45 | WLAN and WiMAX |
| | Thickness | array | array | array | | |
| | | 3.55 | –29.55 | 224 | | |
| | 1.5 mm | For 5 * 8 cell | For 5 * 8 cell | For 5 * 8 cell | | |
| | | array | array | array | | |
| | | 3.575 | –33.10 | 135 | | |
| [54] | 26 * 40 * 0.64 | 4.5 | –41 | 200 | 4–6 | WLAN applications |
| | | | | 100 | | |
| [55] | 27.2 * 16.2 * 1 | 2.45 | –25 | 715 | --- | WLAN applications |
| | | 5.8 | –25 | 1017 | | |
| | | 2.400 | –32.846 | 51 | 6.334 | |
| | | 2.414 | –29.554 | 50 | 6.508 | |
| [56] | 60 * 80 * | 2.416 | –24.221 | 48 | 6.394 | WLAN applications |
| | | 2.422 | –24.029 | 53 | 6.372 | |
| | | 2.422 | –30.602 | 53 | 6.404 | |
| [57] | Circular substrate Radius = 46.2 mm Thickness = 2.34 | 2.45 | –23 | 1.2%/0.8%/0.4% | --- | L-band |
| [58] | 40 * 34 * 1.6 | --- | --- | 560 690 | 2.48–4.72 | WiMAX and WLAN band |
| [59] | 40 * 35 * 0.762 | 2.7 | –13.805 | 504 | -- | WiMAX and C-band |
| | | 8.2 | –29.08 | 1207 | | |
| [62] | 38 * 32 * 1.5 | 2.7 | <–18 | 4300 | 1–8 | WiMAX applications |
| | | 5.6 | <–28 | | | |
| [64] | Circular substrate of radius 30.48 mm and thickness 2.032 mm | 2.4 | –25 | --- | 3 | Wi-Fi and GPS |
| [65] | 33 * 50.9 * 0.8 | 3 | <–20 | 370 | 5 (peak) | Wi-Fi and WiMAX |
| | | 4.33 | –26 | 117 | | |
| | | 5.29 | –38 | 185 | | |
| | | 6.256 | –21 | 240 | | |
| [66] | 66.4 * 66.4 * 2 | 7.066 | –16 | 59 | ---- | C- and X-band applications |
| | | 7.846 | –19 | 162 | | |
| | | 8.86 | –16 | 167 | | |
| | | 9.75 | –13 | 138 | | |
| [67] | 120 * 120 * 5 | 3.57 | --- | Narrow | 10.66 (FEM) 12.4 (FDTD) | WiMAX applications |
| [68] | 50 * 35 * 1.5 | 3.51 | –59/–29 | 130/110 | ---- | S- and C-band applications |
| | | 4.86 | –22/–19 | 1170/1270 | | |
| | | 7.8 | 16/–16 | 1360/280 | | |

TABLE 2: Continued.

| Ref. | Dimensions of antenna ($L \times W \times h$) | Resonant frequency (GHz) | Return loss (dB) | Bandwidth (MHz) | Gain (dBi) | Applications |
|--|---|--------------------------|--------------------|------------------|-------------|---|
| [69] | 10 * 8 * 1.6 | 5.57 | <-30 | 780 | 2.3 (peak) | Wireless application at 8.02.11 a/b/g/n/p/h |
| [70] | 43 * 53 * 4.50 | 3.65 | -12.131 | Narrow | 7.267 | GPS, RFID, WiMAX, and HiperLAN applications |
| | | 5.8 | -20.754 | | 7.455 | |
| [71] | 40 * 50 * 0.49 | 4.95 | -20 | 1% | 5.6 | WLAN applications |
| | | 5.3 | (maximum) | 1.2% | 5.9 | |
| [72] | 38 * 25 * 1.6 | 2.5 | -50 (maximum) | 3600 | 2.85 | WLAN and WiMAX band applications |
| | | 3.8 | | | | |
| | | 5.65 | | | | |
| [73] | 27 * 25 * 1.6 | 2.25 | -30 | 980 | 1.97 | WLAN and WiMAX applications |
| | | 3.5 | (maximum) | | 2.45 | |
| | | 5.25 | | | 2.98 | |
| [74] | Antenna 1 35 * 38 * 1 | 1.8 | -25 (maximum) | 60 | ---- | WLAN and WiMAX |
| | Antenna 2 35 * 38 * 1 | 3.5 | | 1520 | | |
| | | 5.8 | | 120 | | |
| Metamaterial-inspired CSRR loaded antennas | | | | | | |
| [75] | 60 * 50 * 1.6 | 1.72 | <-30 | 28.5%/ | 1.2/1.5 | GPS, WCDMA, and GSM1800 |
| | | 3 | <-10 | 8.7% | | |
| [76] | 44.5 * 31.7 * 0.8 | 5.4-5.8 | -22.5 | 400 | 5.33 | WLAN and WiMAX |
| [77] | 50 * 54 * 1.5 | 5.15/6.75 | -20 | Narrow | 6.1/8.2 | WLAN |
| [78] | 73 * 65.6 * 3.2 | 7.5 | -18.9 | 761 | 8.1 | C-band applications |
| [79] | 30 * 34 * 1.6 | 5.8 | -32 | 100 | ---- | IOT band applications |
| | | 5.3 | -13 | 95 | 6.1 | |
| [80] | 40 * 40 * 1.7 | 5.4 | -37 | 105 | 7.3 | WLAN |
| | | | -41 | 140 | | |
| [81] | 30 * 30 * 0.8 | 2.9 | -20 | 600 | 2.2 | WiMAX and BWLAN |
| | | 6.5 | -20 | 2000 | 3.6 | |
| [82] | 14 * 6 * 1.6 | 0.8-2.40 | <-30 at 1.6 GHz | 1600 | 1.5 (peak) | UHF and L-band, S-band |
| | | 0.9-2.3 | | 1400 | | |
| | | 1.725 | | | | |
| [83] | 40 * 40 * 1.6 | 2.075 | -13/-18 | Narrow | 6 (peak) | GSM1800 and X-band |
| | | 1.95 | | | | |
| | | 1.675 | | | | |
| [84] | 21.57 * 25.62 * 1.6 | 2.36 | <-20 | 110 | -- | WLAN and WiMAX |
| | | 4.45 | | 2210 | | |
| | | 3.18 | -10.71 | 25 | 1.9/10.9/ | |
| | | 4.34 | -13.25 | 140 | 1.89/6.28/ | |
| | | 5.1 | -23.11 | 142 | 5.79/9.88/ | |
| [85] | 60 * 60 * 1.6 | 7.04 | -24.13 | 120 | 4.16 | Multiband |
| | | 7.71 | -23.5 | 120 | | |
| | | 9.3 | -15.26 | 135 | | |
| | | 10.12 | -20.99 | 121 | | |
| | | 1.88 | -12 | 50 | 1.46 (peak) | GSM and WLAN |
| [86] | 19.8 * 22.64 * 1.6 | 2.94 | -19 | 90 | 1.62 (peak) | |
| | | 5.5 | -13 | 1820 | 2.68 (peak) | |
| | Antenna 1 20 * 30 * 1.6 | Antenna 1 3.2-3.9 | -50 (maximum) | Antenna 1 700 | ---- | WiMAX and WLAN |
| [87] | Antenna 2 35 * 35 * 1.6 | Antenna 2 5.75-5.85 | | 100 | | |
| | | Antenna 2 2.3-2.48 | -40 (maximum) | Antenna 2 180 | | |
| | | 3.3-4.2 | | 900 | | |
| | | 5.15-5.65 | | 500 | | |

TABLE 2: Continued.

| Ref. | Dimensions of antenna ($L \times W \times h$) | Resonant frequency (GHz) | Return loss (dB) | Bandwidth (MHz) | Gain (dBi) | Applications |
|------|---|--------------------------|--------------------|-----------------|------------|---|
| [88] | 40 * 35 * 1.6 | 2.28 | -10.71 | 160 | 2.16 | WLAN, WiMAX, and X-band applications |
| | | 2.65 | -11.20 | 150 | 1.91 | |
| | 30 * 24.8 * 1.6 | 4.80 | -23.23 | 440 | 2.65 | |
| | | 5.89 | -17.15 | 320 | 2.81 | |
| | | 8.73 | -13.69 | 470 | 3.01 | |
| [89] | 24.3 * 30.8 * 3.2 | 3.85 | -20 -25 | Wide bandwidth | 3 | WLAN, X-band, and ku-band |
| | | 2.4 | | 15.1% | 3.48 | |
| | | 3.48 | | 3.45% | 3.02 | |
| | | 4.02 | | 12.59% | 4.49 | |
| [90] | 40 * 40 * 1.5748 | 4.34 | -35 (maximum) | 3.33% | 4.25 | WiMAX, weather radar system, PAN, and lower WLAN applications |
| | | 5.1 | | 3.25% | 3.59 | |
| | | 5.54 | | 5.4% | 3.81 | |
| | | 6.24 | | 16.58% | 5 | |
| | | 2.36 | | 1000 | 3.63 | |
| [91] | 24.72 * 22.8 * 1.6 | 8.45 | <-45 | 1440 | 1 | WLAN and ITU band applications |
| | | | | | | |
| [92] | 47 * 38 * 0.813 | 2.3-11.5 | -43.5 (maximum) | 9200 | 3.3 (peak) | UWB |
| [93] | 30 * 31 * 1.6 | 2.5 | -23 | 200 390 | 2.25 | Bluetooth, WLAN, and WiMAX |
| [94] | 24 * 30 * 1.6 | 2.86-12.2 | -45 (maximum) | Wide bandwidth | 6.45 | UWB applications |
| [95] | 38 * 40 * 0.8 | 2.85-12.0 | -30 (maximum) | Wide bandwidth | <5 | UWB applications |

The present study is really very useful for the researchers working in the direction of 6G communication as for 6G communication it is expected to have data transmission rate of few TBps. In this regard, it is very essential to build certain receiver and transmitter or antennas which are capable of transferring the data with this kind of speed. So, metamaterials possess the potential and with future research there are certain other advancements or improvements are being done. They carry potential to fulfil the need of 6G communication in this field. Metamaterial uses include public safety, sensor detection, high-frequency battlefield communication, augmenting ultrasonic sensors, solar power management, high-gain antennas, and remote aerospace applications.

5. Future Work

Several studies utilized significantly reduced antenna dimensions and constructions that were incredibly small in proportion to the wavelength. Due to their restrictions, electrically small antennas are difficult to design and necessitate trade-offs between antenna size and performance (i.e., bandwidth, efficiency, gain, radiation pattern, etc.). While metamaterials have been shown to be effective at shrinking the size of radiators by enabling novel resonant modes (i.e., ZOR antennas), the fundamental difficulties remain the same. For example, the narrowband properties of metamaterials have a direct effect on the bandwidth of small metaresonator antennas. Additionally, the majority of designs concentrated only on

reducing the size of the antenna through the utilisation of metamaterial cells' subwavelength resonance, but they did not enhance the antenna's overall performance. Specifically, the interaction between the metamaterial cell and the remainder of the antenna (e.g., monopole and patch) was ignored, despite the fact that this interaction is critical for the current distribution, which heavily influences the antenna performance. While designing an MSA with a metaresonator stacking can be uncomplicated, achieving a high overall performance involves additional considerations such as the feeding method, metamaterial type, location of the unit cells, and shape of the main antenna body. As a result, we believe that metamaterials can expedite and aid in the design of MSAs, but additional research is necessary.

In order to improve antenna properties, there is also a strong need for theoretical formulations which will serve as design recommendations. Clearly, the field is not mature yet, and while there are some excellent examples of metamaterial antennas, scientific understanding of the underlying concepts is limited, and designs are largely based on electromagnetic simulations. As a result, it is vital to develop a sound theory for metamaterial-inspired antennas in order to expedite the design process and eventually improve performance. Metamaterial-based strategies for enhancing the restricted bandwidth and low efficiency of MSAs are critical for future communications. Small, power-efficient, wide-band antennas will become increasingly important as bandwidths increase, devices get more compact, and SNR becomes the dominant metric for future 5G or 6G and beyond networks.

6. Conclusion

This paper has explained the various metamaterial-inspired MPA along with band rejected characteristics. The main venture of this article is to understand the effect of inclusion of various metamaterial structures such as SRR, CSRR, SCSRR, and TSRR on the antenna characteristics. It can be contemplated from the above discussion that most of the metamaterial structures have severely reduced the size of the traditional antenna along with the desired antenna characteristics, but in few designs of metamaterial-inspired antenna, performance parameters of antenna are being compromised. The most important thing is that antenna's performance parameters, for example, impedance matching, gain, and return loss, should not be compromised while designing a miniaturized antenna. The metamaterial structures can be incorporated in the conventional patch antenna to improve the antenna performances. The present survey has identified landmark outcomes such as enhancement of impedance bandwidth of conventional antenna, improvement in gain, and band notching of ultrawideband antennas. To conclude, all the above described techniques to improve the antenna performances such as enhancement of bandwidth and notching of band pass frequencies have its own significance in designing the metamaterial-inspired antennas. These approaches have their own set of design constraints that need be addressed in future antenna designs. However, these metamaterial-inspired antennas become suitable for various wireless applications such as GSM, WiMAX, WLAN, RFID, satellite communication, ISM band, and radar.

In comparison to previous generations of wireless communication networks, the sixth-generation (6G) modern communication systems are expected to be revolutionary, progressing from "connected things" to "connected intelligence," with more stringent requirements such as extremely high data rates, extreme energy efficiency, massive low latency control, extremely broad radio frequencies, pervasive uninterrupted global network coverage, and connected intelligence. Artificial intelligence (AI) is a feasible technology for next-generation networks due to its ability to meet the aforementioned requirements. AI has been used as a novel paradigm for designing and optimizing 6G networks with high-level intelligence. It can be used to handle NP difficulties, such as the uncertain, time-variant, and intricate properties of 6G. On the other hand, 6G places a premium on security and privacy, as hostile and malicious operations have the potential to cause devastating network damage. Due to the rapid growth of smart terminals and infrastructure, as well as applicability (e.g., virtual and augmented reality, remote surgery, and holographic projection) with a variety of requirements, current networks (e.g., 4G and 5G networks) may be unable to fully meet rapidly increasing traffic demands.

Data Availability

The data used to support the findings of this study are available from the corresponding author upon request.

Conflicts of Interest

The authors declare that there are no conflicts of interest regarding the publication of this paper.

References

- [1] C. Balanis, *Antenna Theory Analysis and Design*, John Wiley & Sons, New York, NY, USA, 1982.
- [2] R. Garg, *Microstrip Antenna Design Handbook*, Artech House, Boston, Mass; London, 2001.
- [3] K. Jairath, N. Singh, V. Jagota, and M. Shabaz, "Compact ultrawide band metamaterial-inspired split ring resonator structure loaded band notched antenna," *Mathematical Problems in Engineering*, vol. 2021, Article ID 5174455, 12 pages, 2021.
- [4] J. Bholra and S. Soni, "Information theory-based defense mechanism against DDOS attacks for WSN," *Lecture Notes in Electrical Engineering*, vol. 683, pp. 667–678, 2021.
- [5] G. A. Deschamps, "Microstrip microwave antennas," in *Proceedings of the 3rd USAF Symposium on Antennas*, IL, USA, October 1953.
- [6] R. Munson, "Conformal microstrip antennas and microstrip phased arrays," *IEEE Transactions on Antennas and Propagation*, vol. 22, no. 1, pp. 74–78, 1974.
- [7] J. Howell, "Microstrip antennas," *IEEE Transactions on Antennas and Propagation*, vol. 23, no. 1, pp. 90–93, 1975.
- [8] N. X. Anusha, S. Vimal, and V. Jackins, "DSA-based secured communication in 5G vehicular networks using edge computing," in *Computational Intelligence in Pattern Recognition*, pp. 389–400, Springer, Berlin, Germany, 2022.
- [9] S. Saralch, V. Jagota, D. Pathak, and V. Singh, "Response surface methodology based analysis of the impact of nanoclay addition on the wear resistance of polypropylene," in *The European Physical Journal - Applied Physics*, J.-M. Nunzi, R. Bennacer, M. El Ganaoui, and M. El Jouad, Eds., vol. 86, no. 1, EDP Sciences, Article ID 10401, 2019.
- [10] Q. Yao, M. Shabaz, T. K. Lohani, M. Wasim Bhatt, G. S. Panesar, and R. K. Singh, "3D modelling and visualization for vision-based vibration signal processing and measurement," *Journal of Intelligent Systems*, vol. 30, no. 1, pp. 541–553, 2021.
- [11] G. Laput, C. Yang, R. Xiao, A. Sample, and C. Harrison, "EM-sense: touch recognition of uninstrumented, electrical and electromechanical objects," in *Proceedings of the 28th Annual ACM Symposium on User Interface Software & Technology*, New York, NY, USA, November 2015.
- [12] A. S. Sappal, "DESIGN of RECTANGULAR MICROSTRIP PATCH ANTENNA USING PARTICLE SWARM OPTIMIZATION," *Computer Science Business*, vol. 2, no. 7, pp. 2918–2920, 2013.
- [13] M. M. Ahamed, K. Bhowmik, and A. A. Suman, "Analysis and design of rectangular microstrip patch antenna on different resonant frequencies for pervasive wireless communication," *International Journal of Scientific and Technology Research*, vol. 1, no. 5, pp. 108–111, 2012.
- [14] V. G. Veselago, "Electrodynamics of media with simultaneously negative electric permittivity and magnetic permeability," in *Advances in Electromagnetics of Complex Media and Metamaterials*, pp. 83–97, Springer Netherlands, Berlin, Germany, 2002.
- [15] Z. Jakšić, S. Vuković, J. Matovic, and D. Tanasković, "Negative refractive index metasurfaces for enhanced biosensing," *Materials*, vol. 4, pp. 1–36, 2010.

- [16] A. Ishimaru, S. Jaruwatanadilok, and Y. Kuga, "Generalized surface plasmon resonance sensors using metamaterials and negative index materials," *The Electromagnetics Academy*, vol. 51, pp. 139–152, 2005.
- [17] M. Shamonin, O. Radkovskaya, C. J. Stevents et al., "Waveguide and sensor systems comprising metamaterial element," in *Proceedings of the DPG—Spring Meeting of the Division Condensed Matter*, pp. 114–118, Regensburg, Germany, March 2006.
- [18] D. Shreiber, M. Gupta, and R. Cravey, "Comparative study of 1-D and 2-D metamaterial lens for microwave nondestructive evaluation of dielectric materials," *Sensors and Actuators A: Physical*, vol. 165, no. 2, pp. 256–260, 2011.
- [19] S. He, Y. Jin, Z. Ruan, and J. Kuang, "On subwavelength and open resonators involving metamaterials of negative refraction index," in *New Journal of Physics*, vol. 7, p. 210, IOP Publishing, 2005.
- [20] M. Huang and J. Yang, "Microwave sensor using metamaterials," in *Wave Propagation InTech*, PR China, 2011.
- [21] N. I. Zheludev, "The road ahead for metamaterials," *Science*, vol. 328, no. 5978, pp. 582–583, 2010.
- [22] V. Jagota and R. K. Sharma, "Interpreting H13 steel wear behavior for austenitizing temperature, tempering time and temperature," *Journal of the Brazilian Society of Mechanical Sciences and Engineering*, vol. 40, 2018.
- [23] V. Jagota, M. Luthra, J. Bholra, A. Sharma, and M. Shabaz, "A secure energy-aware game theory (SEGaT) mechanism for coordination in WSANs," *International Journal of Swarm Intelligence Research*, vol. 13, no. 2, pp. 1–16, 2022.
- [24] D. R. Smith, S. Schultz, P. Markoš, and C. M. Soukoulis, "Determination of effective permittivity and permeability of metamaterials from reflection and transmission coefficients," *Physical Review B*, vol. 65, no. 19, Article ID 195104, 2002.
- [25] S. Wen, Y. Xiang, X. Dai, Z. Tang, W. Su, and D. Fan, "Theoretical models for ultrashort electromagnetic pulse propagation in nonlinear metamaterials," *Physical Review A*, vol. 75, no. 3, Article ID 033815, 2007.
- [26] T. K. Lohani, M. T. Ayana, A. K. Mohammed, M. Shabaz, G. Dhiman, and V. Jagota, "A comprehensive approach of hydrological issues related to ground water using GIS in the Hindu holy city of Gaya, India," *World Journal of Engineering*, p. 6, 2021.
- [27] K. Aydin, K. Guven, and E. Ozbay, "Two-dimensional left-handed metamaterial with a negative refractive index," *Journal of Physics: Conference Series*, vol. 36, pp. 6–11, 2006.
- [28] L. I. Mandelshtam, "Lectures on some problems of the theory of oscillations," *Complete Collection of Works*, vol. 5, pp. 428–467, 1944.
- [29] W. Rotman, "Plasma simulation by artificial dielectrics and parallel-plate media," *IRE Transactions on Antennas and Propagation*, vol. 10, no. 1, pp. 82–95, 1962.
- [30] J. B. Pendry, A. J. Holden, W. J. Stewart, and I. Youngs, "Extremely low frequency plasmons in metallic mesostructures," *Physical Review Letters*, vol. 76, no. 25, pp. 4773–4776, 1996.
- [31] J. B. Pendry, A. J. Holden, D. J. Robbins, and W. J. Stewart, "Magnetism from conductors and enhanced nonlinear phenomena," *IEEE Transactions on Microwave Theory and Techniques*, vol. 47, no. 11, pp. 2075–2084, 1999.
- [32] J. C. Bose, "On the rotation of plane of polarisation of electric wave by a twisted structure," *Proceedings of the Royal Society of London*, vol. 63, no. 389–400, pp. 146–152, 1898.
- [33] D. R. Smith, W. J. Padilla, D. C. Vier, S. C. Nemat-Nasser, and S. Schultz, "Composite medium with simultaneously negative permeability and permittivity," *Physical Review Letters*, vol. 84, no. 18, pp. 4184–4187, 2000.
- [34] J. D. Jackson, *Classical Electrodynamics*, Wiley, New York, NY, USA, 3rd edition, 1999.
- [35] P. B. Dash, B. Naik, J. Nayak, and S. Vimal, "Deep belief network-based probabilistic generative model for detection of robotic manipulator failure execution," in *Soft Computing* Springer Science and Business Media LLC, Berlin, Germany, 2021.
- [36] F. Falcone, T. Lopetegi, J. D. Baena, R. Marques, F. Martin, and M. Sorolla, "Effective negative-/spl epsiv/stopband microstrip lines based on complementary split ring resonators," *IEEE Microwave and Wireless Components Letters*, vol. 14, no. 6, pp. 280–282, 2004.
- [37] M. Naser-Moghadasi, R. A. Sadeghzadeh, T. Sedghi, T. Arbi, and B. S. Virdee, "UWB CPW-fed fractal patch antenna with band-notched function employing folded T-shaped element," *IEEE Antennas and Wireless Propagation Letters*, vol. 12, pp. 504–507, 2013.
- [38] C.-Y. Chen, I.-W. Un, N.-H. Tai, and T.-J. Yen, "Asymmetric coupling between subradiant and superradiant plasmonic resonances and its enhanced sensing performance," *Optics Express*, vol. 17, no. 17, p. 15372, 2009.
- [39] R. Singh, C. Rockstuhl, and W. Zhang, "Strong influence of packing density in terahertz metamaterials," *Applied Physics Letters*, vol. 97, no. 24, 2010.
- [40] R. Melik, E. Unal, N. K. Perkgoz, C. Puttlitz, and H. V. Demir, "Metamaterial based telemetric strain sensing in different materials," *Optics Express*, vol. 18, no. 5, 5000 pages, 2010.
- [41] Z. Djurić, "Mechanisms of noise sources in microelectromechanical systems," *Microelectronics Reliability*, vol. 40, no. 6, pp. 919–932, 2000.
- [42] N. Jacob, M. Kulkarni, and K. Krishnamoorthy, "Omega shaped complementary split ring resonator loaded bandwidth reconfigurable antenna for cognitive radio applications," *Procedia Computer Science*, vol. 171, pp. 1279–1285, 2020.
- [43] C. Saha and J. Y. Siddiqui, "Theoretical model for estimation of resonance frequency of rotational circular split-ring resonators," *Electromagnetics*, vol. 32, no. 6, pp. 345–355, 2012.
- [44] J. D. Baena, J. Bonache, F. Martin et al., "Equivalent-circuit models for split-ring resonators and complementary split-ring resonators coupled to planar transmission lines," *IEEE Transactions on Microwave Theory and Techniques*, vol. 53, no. 4, pp. 1451–1461, 2005.
- [45] K. Jairath and N. Singh, "A novel WLAN and X-Band rejected elliptical slot loaded metamaterial inspired antenna," *Materials Today Proceedings*, 2021.
- [46] Y. Lei, S. Vyas, S. Gupta, and M. Shabaz, "AI based study on product development and process design," in *International Journal of System Assurance Engineering and Management* Springer Science and Business Media LLC, Berlin, Germany, 2021.
- [47] R. K. Garg, J. Bholra, and S. K. Soni, "Healthcare monitoring of mountaineers by low power Wireless Sensor Networks," *Informatics in Medicine Unlocked*, vol. 27, Article ID 100775, 2021.
- [48] D. Qu, L. Shafai, and A. Foroozesh, "Improving microstrip patch antenna performance using EBG substrates," *IEEE Proceedings - Microwaves, Antennas and Propagation*, vol. 153, no. 6, 558 pages, 2006.

- [49] H. Boutayeb and T. A. Denidni, "Gain enhancement of a microstrip patch antenna using a cylindrical electromagnetic crystal substrate," *IEEE Transactions on Antennas and Propagation*, vol. 55, no. 11, pp. 3140–3145, 2007.
- [50] Z.-B. Weng, Y.-C. Jiao, F.-S. Zhang, Y. Song, and G. Zhao, "A multi-band patch antenna on metamaterial substrate," *Journal of Electromagnetic Waves and Applications*, vol. 22, no. 2–3, pp. 445–452, 2008.
- [51] L.-W. Li, Y.-N. Li, and J. R. Mosig, "Design of a Novel Rectangular Patch Antenna with Planar Metamaterial Patterned Substrate," in *Proceedings of the 2008 International Workshop on Antenna Technology: Small Antennas and Novel Metamaterials*, Chiba, Japan, March 2008.
- [52] Y. Zhang, W. Hong, C. Yu, Z.-Q. Kuai, Y.-D. Don, and J.-Y. Zhou, "Planar ultrawideband Antennas with multiple notched bands based on etched slots on the patch and/or split ring resonators on the feed line," *IEEE Transactions on Antennas and Propagation*, vol. 56, no. 9, pp. 3063–3068, 2008.
- [53] N. Singh, S. Singh, and R. K. Sarin, "Effect of Photonic Band Gap Structure on Planar Antenna Configuration," in *othe 2010 10th mediterranean microwave symposium(mms)*, Guzelyurt, Northern Cyprus, August 2010.
- [54] S. S. Pattnaik, J. G. Joshi, S. Devi, and M. R. Lohokare, "Electrically Small rectangular microstrip patch antenna loaded with metamaterial," in *Proceedings of the 9th international symposium on antennas, propagation and em theory. em theory (isape - 2010)*, Guangzhou, China, November 2010.
- [55] N. Singh and S. Singh, "Effect of different structural parameters on Bandwidth and Resonant frequency of Novel MTM," in *Proceedings of the 9th international symposium on antennas, propagation and em theory. em theory (isape 2010)*, Guangzhou, China, November 2010.
- [56] G. Bertin, B. Piovano, R. Vallauri, F. Bilotti, and L. Vegni, "Metamaterial-Inspired Antennas for Telecommunication Applications," in *Proceedings of the 2012 6th European Conference on Antennas and Propagation (EUCAP)*, Prague, Czech Republic, March 2012.
- [57] M.-C. Tang, S. Xiao, T. Deng et al., "Compact UWB antenna with multiple band-notches for WiMAX and WLAN," *IEEE Transactions on Antennas and Propagation*, vol. 59, no. 4, pp. 1372–1376, 2011.
- [58] H. Nornikman, B. H. Ahmad, M. Z. A. Abd Aziz, and A. R. Othman, "Effect of Single Complimentary Split Ring Resonator Structure on Microstrip Patch Antenna design," in *Proceedings of the 2012 ieee symposium on wireless technology and applications (iswta)*, Bandung, Indonesia, September 2012.
- [59] R. O. Ouedraogo, E. J. Rothwell, A. R. Diaz, K. Fuchi, and A. Temme, "Miniaturization of patch antennas using a metamaterial-inspired technique," *IEEE Transactions on Antennas and Propagation*, vol. 60, no. 5, pp. 2175–2182, 2012.
- [60] M. M. Sharma, A. Kumar, S. Yadav, and Y. Ranga, "An ultrawideband printed monopole antenna with dual band-notched characteristics using DGS and SRR," *Procedia Technology*, vol. 6, pp. 778–783, 2012.
- [61] H. Kumar, M. D. Upadhayay, S. M. T. Amita, A. Agarwal, N. Singh, and S. Singh, "A Single Band Notched CPW Antenna design," in *othe 2012 international conference on computer communication and informatics*, Coimbatore, India, January 2012.
- [62] T. Chen, S. Li, and H. Sun, "Metamaterials application in sensing," *Sensors*, vol. 12, no. 3, pp. 2742–2765, 2012.
- [63] S. K. Patel and Y. Kosta, "Investigation on radiation improvement of corner truncated triband square microstrip patch antenna with double negative material," *Journal of Electromagnetic Waves and Applications*, vol. 27, no. 7, pp. 819–833, 2013.
- [64] S. Gupta and G. Mumcu, "A small complementary split ring resonator loaded circularly polarized patch antenna," in *othe 2013 international symposium on electromagnetic theory*, pp. 94–96, Hiroshima, Japan, May 2013.
- [65] A. Kurniawan and S. Mukhlisin, "Wideband Antenna design and fabrication for modern wireless communications systems," *Procedia Technology*, vol. 11, pp. 348–353, 2013.
- [66] S. K. Patel and Y. Kosta, "Complementary split ring resonator metamaterial to achieve multifrequency operation in microstrip-based radiating structure design," *Journal of Modern Optics*, vol. 61, no. 3, pp. 249–256, 2014.
- [67] J. J. Wang, L. L. Gong, Y. X. Sun, Z. P. Zhu, and Y. R. Zhang, "High-gain composite microstrip patch antenna with the near-zero-refractive-index metamaterial," *Optik*, vol. 125, no. 21, pp. 6491–6495, 2014.
- [68] S. K. Patel and Y. P. Kosta, "Metamaterial superstrate-loaded meandered microstrip-based radiating structure for bandwidth enhancement," *Journal of Modern Optics*, vol. 61, no. 11, pp. 923–930, 2014.
- [69] Md. Islam, M. Islam, Md. Samsuzzaman, M. Faruque, N. Misran, and M. Mansor, "A miniaturized antenna with negative index metamaterial based on modified SRR and CLS unit cell for UWB microwave imaging applications," *Materials*, vol. 8, no. 2, pp. 392–407, 2015.
- [70] D. Mitra, B. Ghosh, A. Sarkhel, and S. R. Bhadra Chaudhuri, "A miniaturized ring slot antenna design with enhanced radiation characteristics," *IEEE Transactions on Antennas and Propagation*, vol. 64, no. 1, pp. 300–305, 2016.
- [71] N. Ortiz, J. C. Iriarte, G. Crespo, and F. Falcone, "Design and implementation of dual-band antennas based on a complementary split ring resonators," *Waves in Random and Complex Media*, vol. 25, no. 3, pp. 309–322, 2015.
- [72] P. Dawar, N. S. Raghava, and A. De, "A novel metamaterial for miniaturization and multi-resonance in antenna," *Cogent Physics*, vol. 2, no. 1, Article ID 1123595, 2015.
- [73] V. Rajeshkumar and S. Raghavan, "A compact metamaterial inspired triple band antenna for reconfigurable WLAN/WiMAX applications," *AEU - International Journal of Electronics and Communications*, vol. 69, no. 1, pp. 274–280, 2015.
- [74] C. Zhu, T. Li, K. Li et al., "Electrically small metamaterial-inspired tri-band Antenna with meta-mode," *IEEE Antennas and Wireless Propagation Letters*, vol. 14, pp. 1738–1741, 2015.
- [75] M. Rahimi, M. Maleki, M. Soltani, A. S. Arezomand, and F. B. Zarrabi, "Wide band SRR-inspired slot antenna with circular polarization for wireless application," *AEU - International Journal of Electronics and Communications*, vol. 70, no. 9, pp. 1199–1204, 2016.
- [76] T. Alam, M. Samsuzzaman, M. R. I. Faruque, and M. T. Islam, "A metamaterial unit cell inspired antenna for mobile wireless applications," *Microwave and Optical Technology Letters*, vol. 58, no. 2, pp. 263–267, 2015.
- [77] X.-J. Gao, T. Cai, and L. Zhu, "Enhancement of gain and directivity for microstrip antenna using negative permeability metamaterial," *AEU - International Journal of Electronics and Communications*, vol. 70, no. 7, pp. 880–885, 2016.

- [78] N. Singla and A. Rajput, "Compact Dual-Band Metamaterial-Inspired Antenna Using SCSRR Structures for mobile applications," in *Proceedings of the 2016 11th international conference on industrial and information systems (iciis)*, Roorkee, India, December 2016.
- [79] S. Muzeeb, G. S. Rajesh, and V. Kumar, "Design of a Quadruple Band Printed Monopole Antenna Using ENG Metamaterial antenna," in *othe 2016 ieee international conference on recent trends in electronics, information & communication technology (rteict)*, Bangalore, India, May 2016.
- [80] R. Rajkumar and K. Usha Kiran, "A compact metamaterial multiband antenna for WLAN/WiMAX/ITU band applications," *AEU - International Journal of Electronics and Communications*, vol. 70, no. 5, pp. 599–604, 2016.
- [81] M. Ameen, R. Kumar, N. Mishra, and R. K. Chaudhary, "A Compact Triple Band Dual Polarized Metamaterial Antenna Loaded with Double Hexagonal SRR for WLAN/WiMAX Applications," in *Proceedings of the 2017 ieee international conference on antenna innovations & modern technologies for ground, aircraft and satellite applications (iaim)*, Bangalore, India, November 2017.
- [82] A. Yadav, S. Agrawal, and R. P. Yadav, "SRR and S-shape slot loaded triple band notched UWB antenna," *AEU - International Journal of Electronics and Communications*, vol. 79, pp. 192–198, 2017.
- [83] S. Heydari, K. Pedram, Z. Ahmed, and F. B. Zarrabi, "Dual band monopole antenna based on metamaterial structure with narrowband and UWB resonances with reconfigurable quality," *AEU - International Journal of Electronics and Communications*, vol. 81, pp. 92–98, 2017.
- [84] R. Samson Daniel, R. Pandeeswari, and S. Raghavan, "Multiband monopole antenna loaded with complementary split ring resonator and C-shaped slots," *AEU - International Journal of Electronics and Communications*, vol. 75, pp. 8–14, 2017.
- [85] R. Rajkumar and K. Usha Kiran, "A metamaterial inspired compact open split ring resonator antenna for multiband operation," *Wireless Personal Communications*, vol. 97, no. 1, pp. 951–965, 2017.
- [86] C. Arora, S. S. Pattnaik, and R. N. Baral, "Performance enhancement of patch antenna array for 5.8 GHz Wi-MAX applications using metamaterial inspired technique," *AEU - International Journal of Electronics and Communications*, vol. 79, pp. 124–131, 2017.
- [87] V. R. Nuthakki and S. Dhamodharan, "UWB Metamaterial-based miniaturized planar monopole antennas," *AEU - International Journal of Electronics and Communications*, vol. 82, pp. 93–103, 2017.
- [88] N. Saravanan, V. B. Gao, and S. M. Umarani, "Gain enhancement of patch antenna integrated with metamaterial inspired superstrate," *Journal of Electrical Systems and Information Technology*, vol. 5, no. 3, pp. 263–270, 2018.
- [89] M. Venkateswara Rao, B. T. P. Madhav, T. Anilkumar, and B. Prudhvi Nadh, "Metamaterial inspired quad band circularly polarized antenna for WLAN/ISM/Bluetooth/WiMAX and satellite communication applications," *AEU - International Journal of Electronics and Communications*, vol. 97, pp. 229–241, 2018.
- [90] M. Labidi and F. Choubani, "Performances enhancement of metamaterial loop antenna for terahertz applications," *Optical Materials*, vol. 82, pp. 116–122, 2018.
- [91] D. Chaturvedi and S. Raghavan, "A compact metamaterial-inspired antenna for WBAN application," *Wireless Personal Communications*, vol. 105, no. 4, pp. 1449–1460, 2019.
- [92] Md. Hasan, M. Rahman, M. Faruque, M. Islam, and M. Khandaker, "Electrically compact SRR-loaded metamaterial inspired quad band Antenna for bluetooth/WiFi/WLAN/WiMAX system," *Electronics*, vol. 8, no. 7, 790 pages, 2019.
- [93] V. N. K. R. Devana and A. M. Rao, "Compact UWB monopole antenna with quadruple band notched characteristics," *International Journal of Electronics*, vol. 107, no. 2, pp. 175–196, 2019.
- [94] S. Luo, Y. Chen, D. Wang, Y. Liao, and Y. Li, "A monopole UWB antenna with sextuple band-notched based on SRRs and U-shaped parasitic strips," *AEU - International Journal of Electronics and Communications*, vol. 120, Article ID 153206, 2020.
- [95] N. Sharma and S. S. Bhatia, "Design of printed monopole antenna with band notch characteristics for ultra-wideband applications," *International Journal of RF and Microwave Computer-Aided Engineering*, vol. 29, no. 10, 2019.
- [96] M. Elhabchi, M. Srifi, and R. Touahni, "A Metamaterial inspired elliptical slotted antenna for WLAN and uplink/downlink X-bands Rejection," in *Proceedings of the third international conference on computing and wireless communication systems, iccwcs 2019*, Ibn Tofail University -Kénitra- Morocco, April 2019.
- [97] S. Thakur and N. Singh, "Design of a circular-slot multiband (UWB) antenna with non-periodic DGS for WLAN/WiMAX applications," *Journal of Physics: Conference Series*, vol. 1579, no. 1, Article ID 012011, 2020.
- [98] S. Alotaibi and A. A. Alotaibi, "Design of a planar tri-band notch UWB antenna for X-band, WLAN, and WiMAX," *Engineering, Technology & Applied Science Research*, vol. 10, no. 6, pp. 6557–6562, 2020.
- [99] A. A. Althuwayb, "Enhanced radiation gain and efficiency of a metamaterialinspired wideband microstrip antenna using substrate integrated waveguide technology for sub-6 GHz wireless communication systems," *Microw Opt Technol Lett*, vol. 63, pp. 1892–1898, 2021.
- [100] S. Prasad Jones Christydass and N. Gunavathi, "OCTA-BAND metamaterial inspired multiband monopole antenna for wireless application," *Progress In Electromagnetics Research C*, vol. 113, pp. 97–110, 2021.